

In situ temperature control of molecular beam epitaxy growth using band-edge thermometry

Shane Johnson, Chau-Hong Kuo, Martin Boonzaayer, Wolfgang Braun, Ulrich Koelle, Yong-Hang Zhang, and John Roth

Citation: *Journal of Vacuum Science & Technology B* **16**, 1502 (1998); doi: 10.1116/1.589975

View online: <http://dx.doi.org/10.1116/1.589975>

View Table of Contents: <http://scitation.aip.org/content/avs/journal/jvstb/16/3?ver=pdfcov>

Published by the AVS: Science & Technology of Materials, Interfaces, and Processing

Articles you may be interested in

[Molecular beam epitaxy of InP-based alloys for long-wavelength vertical cavity lasers](#)

J. Vac. Sci. Technol. B **24**, 1544 (2006); 10.1116/1.2200380

[GaAs-based room-temperature continuous-wave 1.59 \$\mu\$ m GaInNAsSb single-quantum-well laser diode grown by molecular-beam epitaxy](#)

Appl. Phys. Lett. **87**, 231121 (2005); 10.1063/1.2140614

[Fabrication of a substrate-independent aluminum oxide-GaAs distributed Bragg reflector](#)


Appl. Phys. Lett. **75**, 1371 (1999); 10.1063/1.124697

[Growth and characterization of defect-free GaAs/AlAs distributed Bragg reflector mirrors on patterned InP-based heterostructures](#)





J. Vac. Sci. Technol. B **16**, 1417 (1998); 10.1116/1.589958

[Substrate temperature measurement by absorption-edge spectroscopy during molecular beam epitaxy of narrow-band gap semiconductor films](#)

J. Vac. Sci. Technol. B **15**, 329 (1997); 10.1116/1.589316



Instruments for Advanced Science

<p>Contact Hiden Analytical for further details: W www.HidenAnalytical.com E info@hiden.co.uk</p> <p>CLICK TO VIEW our product catalogue</p>	 <p>Gas Analysis</p> <ul style="list-style-type: none"> › dynamic measurement of reaction gas streams › catalysis and thermal analysis › molecular beam studies › dissolved species probes › fermentation, environmental and ecological studies 	 <p>Surface Science</p> <ul style="list-style-type: none"> › UHV TPD › SIMS › end point detection in ion beam etch › elemental imaging - surface mapping 	 <p>Plasma Diagnostics</p> <ul style="list-style-type: none"> › plasma source characterization › etch and deposition process reaction › kinetic studies › analysis of neutral and radical species 	 <p>Vacuum Analysis</p> <ul style="list-style-type: none"> › partial pressure measurement and control of process gases › reactive sputter process control › vacuum diagnostics › vacuum coating process monitoring
---	--	--	--	--

***In situ* temperature control of molecular beam epitaxy growth using band-edge thermometry**

Shane Johnson,^{a)} Chau-Hong Kuo, Martin Boonzaayer, Wolfgang Braun, Ulrich Koelle, and Yong-Hang Zhang

Center for Solid State Electronics Research, Arizona State University, Tempe, Arizona 85287-6206

John Roth

HRL Laboratories, LLC, Malibu, California 90265-4799

(Received 22 December 1997; accepted 27 January 1998)

Band-edge thermometry is becoming an established noncontact method for determining substrate temperature during molecular beam epitaxy. However, with this technique thin-film interference and/or absorption in the growing epilayer can cause shape distortions of the spectrum that may be interpreted erroneously as real temperature shifts of the substrate. An algorithm is presented that uses the width of the spectrum to correct for apparent temperature errors caused by interference and absorption in the epilayer. This correction procedure is tested on substrate temperature data taken during the growth of a $\lambda=930$ nm resonant cavity, where the apparent substrate temperature oscillates ± 5 °C during the growth of the mirror stacks. These oscillations are reduced to ± 3 °C using the correction algorithm. A recently developed model for the substrate temperature dynamics in molecular beam epitaxy shows that roughly ± 1 °C of the remaining ± 3 °C temperature oscillations are real. Band-edge thermometry is also used to control the substrate temperature to within ± 2 °C during the growth of near-lattice-matched InGaAs on InP, whereas the same growth under constant thermocouple temperature would result in a 50 °C rise in the actual substrate temperature. © 1998 American Vacuum Society. [S0734-211X(98)09103-3]

I. INTRODUCTION

As the physical dimensions of semiconductor devices have become progressively smaller and device designs progressively more sophisticated, the requirements for control over the fabrication processes have become more stringent. Substrate temperature is a critical parameter in determining the quality and composition of deposited layers in molecular beam epitaxy (MBE). Recently, several noncontact optical methods that infer substrate temperature from the band gap (or band edge) of the substrate material have been developed. The common implementations of band-edge thermometry are diffuse reflectance spectroscopy (DRS),^{1,2} specular reflectance,³ and transmission spectroscopy.⁴⁻⁶ In these methods the temperature of the substrate is inferred from the band edge (i.e., the onset of transparency) of the substrate. To determine the temperature accurately, a spectral signature is needed that can be related to the position of the band edge, and hence, the temperature.

In the work described in this article we determine the temperature of the substrate from the knee region (solid circles) of the band-edge spectrum shown in Fig. 1, as depicted by the solid circles on the plot of reflectance versus wavelength. The knee region of the spectrum is characterized by a fit to the following expression, which has an asymptotic linear behavior away from the knee:

$$y = y_0 + m_2 \lambda_a \ln \left[1 + \exp \left(\frac{(\lambda - \lambda_k)}{\lambda_a} \right) \right]. \quad (1)$$

^{a)}Corresponding author; electronic mail: shane.johnson@asu.edu

The two fitting parameters λ_k and λ_a are independent of the absolute intensity of the spectrum and can be used to determine temperature. The asymptotes of Eq. (1) are shown in Fig. 1, as line 1 (y_0) and line 2 (which has slope m_2). The intersection of these two lines, λ_k , which defines the location of the band edge, will henceforth be referred to as the “position of the knee.” The curvature or sharpness of the bend in the spectrum at the knee determines λ_a , which is a measure of the width of the spectrum. Henceforth, λ_a will be referred to as the “width of the knee.” λ_k is related to the band-gap energy (or absorption-edge position) and λ_a is related to the Urbach parameter (or absorption-edge width).^{7,8}

II. EXTRACTING TEMPERATURE FROM THE BAND-EDGE SPECTRUM

In band-edge thermometry, substrate temperature is typically inferred from the position of the spectrum using a previously determined calibration curve. Since the position of the band-edge spectrum depends on the physical properties of the substrate,^{7,8} one has to make a separate calibration curve for each set of wafers with a different thickness or a different back-surface texture, even though the substrate material is identical. Therefore, a more general way to get temperature from the spectra is needed.

For direct-band-gap semiconductor materials such as GaAs and InP, that have an exponential absorption edge (or Urbach edge),⁹ the relationship between the position and the width of the knee of a calibration wafer and the position and the width of the knee of the measured substrate is given by^{7,8}

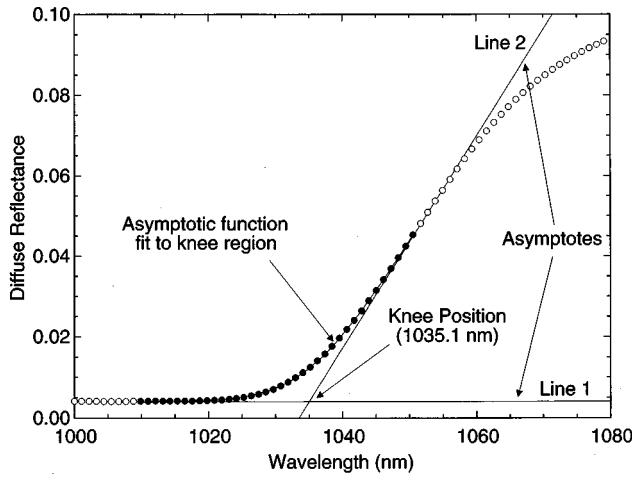


FIG. 1. Illustration of a fit of an asymptotic function to the knee region of the diffuse reflection spectrum, showing the position of the knee in the spectrum.

$$\frac{1}{\lambda_k} = \frac{1}{\lambda_k^{\text{cal}}} - \frac{E_0}{hc} \ln \left[\frac{\lambda_a a_0 d}{\lambda_a^{\text{cal}} a_0^{\text{cal}} d^{\text{cal}}} \left(\frac{\lambda_k^{\text{cal}}}{\lambda_k} \right)^2 \right]. \quad (2)$$

In Eq. (2), E_0 is the Urbach parameter (or width of the absorption edge), d is substrate thickness, and a_0 is 1 for transmission measurements and 2 for diffuse reflection measurements. (Diffuse reflection is equivalent to double-pass transmission.⁸) The term $a_0 d$ accounts for any differences in optical path length inside the substrate. The superscript cal designates parameters that describe the calibration wafer.

Linearizing Eq. (2) (neglecting the higher-order terms in λ_a) and using the relationship $3.6\lambda_a = \lambda_k^2 E_0 / hc$,^{7,8} we get

$$\lambda_k^{\text{cal}} = \lambda_k - \frac{\lambda_k^2 E_0}{hc} \ln \left(\frac{a_0 d}{a_0^{\text{cal}} d^{\text{cal}}} \right) - 3.6[\lambda_a - \lambda_a^{\text{cal}}]. \quad (3)$$

The second term in Eq. (3) corrects for differences in the position of the knee caused by differences in the optical path of the reference and measured substrates. Since the absorption edge is exponential, this correction is given by the natural logarithm of the ratio of the optical path lengths. The third term in Eq. (3) corrects for spurious shifts in the position of the knee that may be caused by any of the following factors: (1) thin-film interference; (2) absorbing overlayers; (3) variations in light scattering at the back of the substrate; (4) higher-order effects of the optical configuration used to determine the band edge; (5) time-dependent variations in the signal from the band edge caused by anisotropic scattering during substrate rotation; and (6) nonuniformities in the optical response of the wavelength selective detection system.^{7,8} In each of these cases a shift in the position of the knee toward lower (higher) energies is accompanied by an increase (decrease) in the width of the knee.

In Eq. (3), $\lambda_k^2 E_0 / hc$ and $3.6\lambda_a^{\text{cal}}$ are linear functions of λ_k , and are approximately equal. The linearity of these two functions arises from the fact that the width and the position of the band edge are linear functions of temperature above room temperature.⁹ Therefore, to first order in λ_a and E_0 ,

the right-hand side of Eq. (3) can be rewritten as a linear function of the position of the knee of the measured substrate:

$$\lambda_k^{\text{cal}} = \lambda_k - A_1(\lambda_k - \lambda_1) \ln \left(\frac{a_0 d}{a_0^{\text{cal}} d^{\text{cal}}} \right) - C_s [3.6\lambda_a - A_2(\lambda_k - \lambda_2)] \quad (4)$$

for GaAs and InP λ_1 and λ_2 are on the order of 1 μm , and A_1 and A_2 are on the order of 0.05.

In practice, the interpretation of band-edge spectra is further complicated if the spectrometer used to record the spectra fails to fully resolve the shape of the spectrum in the region of the knee, as is the case with commercially available band-edge thermometers. Artificial broadening of the spectra reduces the ability of the third term of Eqs. (3) and (4) to adjust for spurious shifts in the position of the knee. Therefore, in order to extend the correction term in Eq. (3) to instruments with less than ideal resolution, an adjustable multiplicative constant, C_s , is used to scale the correction [see Eq. (4)]. $C_s = 1$ in the ideal case and it can be increased to compensate for any reduction in coupling between the width of the knee and the position of the knee when the instrument resolution is below the critical value needed to resolve the band edge of the substrate.

Equation (4) relates the position and the width of the knee of the measured substrate to the position of the knee of the calibration wafer. Using this relationship, substrate temperature can be obtained directly from the previously determined calibration curve, as follows:

$$T = T_1 + T_2 \lambda_k^{\text{cal}} + T_3 (\lambda_k^{\text{cal}})^2. \quad (5)$$

In Eq. (5), T_1 , T_2 , and T_3 are fitting parameters that are determined experimentally. Since the energy shift in the band gap is proportional to the phonon occupation, which is typically linear in temperature for temperatures above room temperature,^{9,10} a linear fit is usually sufficient when the position of the knee is given in terms of energy. Similarly, in terms of wavelength, a second-order fit is usually sufficient. Higher-order fitting parameters can be added to Eq. (5) when the shift of the band edge is less than ideal.

III. SUBSTRATE TEMPERATURE DURING THE GROWTH OF A 930 NM RESONANT CAVITY

In structures such as quarter-wave mirror stacks, thin-film interference can have a large effect on the shape of the spectrum. To test the validity of the correction algorithm derived above, a $\lambda = 930$ nm distributed Bragg reflector (DBR) resonant cavity, comprising a ten period 65.4 nm thick GaAs by 77.8 nm thick $\text{Al}_{0.98}\text{Ga}_{0.02}\text{As}$ quarter-wave stack on each side of a 261.6 nm thick GaAs cavity is grown. This structure is grown on a radiatively heated 50 mm diam semi-insulating GaAs substrate, in a Vacuum Generators (VG) V80H MBE system. Substrate temperature is controlled by holding constant the temperature (766 °C) of the thermocouple located between the substrate heater and the substrate in the V80H sample manipulator.

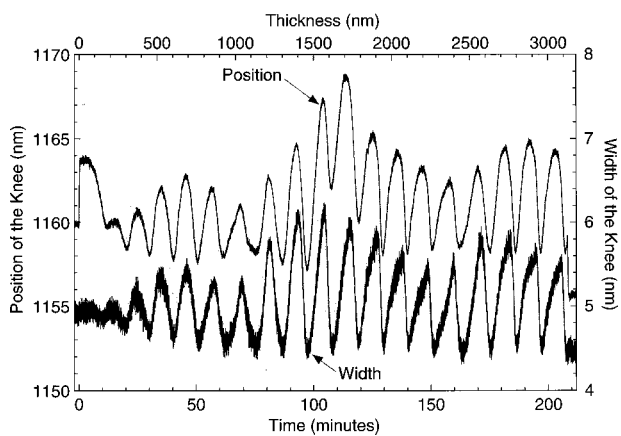


FIG. 2. Oscillations in the position and the width of the knee of the diffuse reflectance spectrum during the growth of a ten-period distributed Bragg reflector pair with a $\lambda=930$ nm resonant cavity. For clarity, the cavity structure is drawn behind the data.

The width and the position of the knee of the diffuse reflectance spectra taken during this growth are shown in Fig. 2. To put this data in perspective, the resonant cavity structure is superimposed over the data, where the shaded layers are GaAs. Growth began at 0 min and ended at 208.4 min. During this time, interference effects cause the position and the width of the knee of the spectrum to oscillate. During growth, the peaks and valleys of the interference fringe spectrum move through the knee region of the band-edge spectrum, broadening and narrowing this region of the spectrum. As the structure thickens, the interference fringes get closer together, increasing the distortion of the knee region of the spectrum. The result is a general increase in the amplitude of the oscillations with structure thickness. Initially, the interference fringes are broad, and affect the knee region of the spectrum in a linear manner. Consequently, the position and the width of the knee oscillate in phase. However, during the latter part of the growth the fringes become narrow, and affect the knee region of the spectrum in a nonlinear manner, which causes the position and the width of the knee to oscillate out of phase. This eventually reduces the effectiveness of the correction algorithm in Eq. (4).

The temperature of the substrate as determined using DRS during the growth of the resonant cavity is shown in Fig. 3. The curve labeled “uncorrected” is the temperature given by the calibration curve [Eq. (5)] when using the position of the knee in the measured spectrum. The curve labeled “corrected” is the temperature given by the calibration curve when the position of the knee is adjusted for variations in the width of the knee [see Eq. (4)]. For clarity, the DBR cavity structure is drawn in the background of Fig. 3 (shaded areas are GaAs). The oscillations in the uncorrected temperature are a result of thin-film interference distortion of the band-edge spectrum, and to a lesser extent, are a result of periodic variations in emission properties of the substrate. In the corrected temperature, most of the spurious temperature shifts caused by thin-film interference have been successfully removed by the correction algorithm.

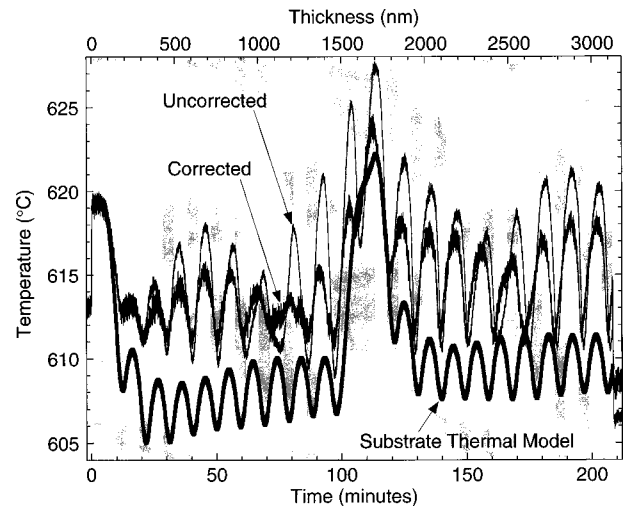


FIG. 3. Substrate temperature inferred from the knee region of the diffuse reflectance spectrum during the growth of a $\lambda=930$ nm resonant cavity structure on semi-insulating GaAs. In the uncorrected curve, temperature is inferred from the position of the knee of the spectrum. In the corrected curve, temperature is inferred from both the position and the width of the knee of the spectrum.

The substrate temperature increases abruptly by about 6°C at the start of growth, when two Ga cells are opened. The first cell (Ga1) contributes a GaAs growth rate of 14.7 nm/min, while the second cell (Ga2) contributes a GaAs growth rate of 0.3 nm/min. The Ga2 cell remains open during the entire growth and supplies the Ga component of the $\text{Al}_{0.98}\text{Ga}_{0.02}\text{As}$ layers. The initial sharp rise in temperature is caused by the additional heat load on the substrate due to radiant energy from the Ga cells. Since the growth is done under constant thermocouple temperature, it appears that the thermocouple is insensitive to this additional heat load.

The substrate temperature stays constant during the growth of the first GaAs layer. At the end of the GaAs layer growth, the Ga1 shutter is closed and the Al shutter is opened (AlAs growth rate of 14.7 nm/min). It is interesting to note that since no sudden temperature changes are observed at the GaAs–AlGaAs interfaces, the heat load of the Al cell and the heat load of the Ga1 cell are roughly the same. During the growth of the first AlGaAs layer the substrate cools as the emittance of the substrate increases with the addition of the lower-index AlGaAs layer. The thermocouple appears to be insensitive to these changes, however, DRS correctly senses the drop in the true substrate temperature. During the growth of the remainder of the first mirror stack the substrate temperature fluctuates around an average temperature of about 613°C .

During the growth of the 261.6 nm GaAs cavity the substrate temperature increases significantly, and at the end of the GaAs cavity the temperature is about 3°C higher than the initial GaAs growth temperature. During the growth of the top mirror stack the substrate again cools, reaching an average temperature of about 615°C for the rest of the growth. This new average temperature is about 2°C higher than that of the first mirror stack. During the growth of the

second mirror, the temperature oscillations (after correction) are larger than in the first stack. In this case, the increase is not real, as the effectiveness of the correction algorithm is reduced by the fact that the position and width of the knee are now slightly out of phase. At the end of the growth, the substrate temperature abruptly drops by about 5 °C when the two Ga shutters are closed.

The two major trends observed in the substrate temperature during the growth of the DBR cavity structure are the decrease in temperature with the growth of AlGaAs on thick GaAs layers and the increase of temperature with the growth of the GaAs cavity on the mirror stack. In both cases the temperature decrease (or increase) is due to the increase (or decrease) in the emittance of the substrate, which is caused by the deposition of a layer whose index of refraction is lower (or higher) than that of the underlying material.

In order to better understand the effect the optical properties of the growing structure have on substrate temperature, a mathematical model for radiant energy transfer between the heater and substrate¹¹ is used to simulate substrate temperature variation during the growth of the structure at constant thermocouple temperature. The result of this simulation is labeled the “substrate thermal model” in Fig. 3. This model does a remarkably good job of reproducing key features of the substrate temperature variation during the growth of the DBR cavity. For example, it correctly predicts: (1) the higher average temperature during the growth of the second mirror stack; (2) the peak temperature during the growth of the GaAs cavity; and (3) the decrease in temperature during the first AlGaAs–GaAs period of each mirror stack.

The substrate thermal model also predicts small temperature oscillations that have the same period as the mirror stack. In comparison, the period of the DRS temperature oscillations is about 1.2 times larger. The longer period for DRS is due to the interference distortion of the band-edge spectrum in the vicinity of the knee wavelength, which is about 20% longer than the wavelength of the resonant cavity. These two different periods result in a beating in the DRS temperature that is particularly noticeable in the first mirror stack. The fact that the period for interference dominates the DRS temperature during the growth of the mirror stacks indicates that the temperature displacement of the diffuse reflectance spectrum is smaller than the interference displacement, even after correction.

The substrate temperature oscillations during the growth of the mirror stacks have maxima in the AlGaAs layers and minima in the GaAs layers. At first this behavior appears to be out of phase with the more prominent features of the temperature curve, namely, that the temperature decreases during AlGaAs growth and increases during GaAs growth. The explanation for this is as follows: Superimposed over the broad subgap emission spectrum of GaAs–AlGaAs materials is a narrow emission peak where the band gap of the material overlaps the tail of the blackbody spectrum. The combination of band-gap changes and interference effects cause the integrated intensity of the emission peak to vary with the same period as the quarter-wave mirror stacks. Because of this,

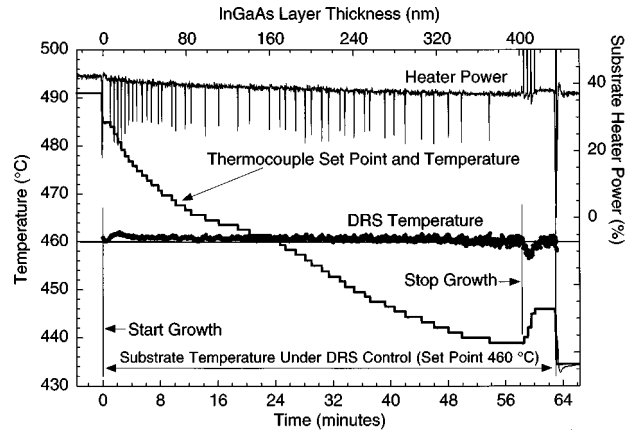


FIG. 4. Feedback control of substrate temperature during the growth of near-lattice-matched InGaAs on semi-insulating InP, using diffuse reflectance spectroscopy (DRS). The substrate setpoint (460 °C), the DRS temperature, the thermocouple temperature and setpoint, and the heater power are shown.

substrate emission goes through a maximum in the 65.4 nm GaAs layers and a minimum in the 77.8 nm AlGaAs layers.

IV. TEMPERATURE CONTROL DURING THE GROWTH OF ABSORBING OVERLAYERS

During the growth of absorbing overlayers, such as near-lattice-matched InGaAs on InP, radiatively heated substrates are known to heat up dramatically as the layer becomes thicker, and this occurs with either constant heater power or constant thermocouple temperature.¹² Under these growth conditions it is imperative that one has an alternative *in situ* method of determining substrate temperature. Band-edge thermometry is a suitable method, with the limitation that the opaque overlayer will eventually obscure the band edge of the substrate.

In the following experiment a near-lattice-matched, 400 nm thick, InGaAs layer is grown on a radiatively heated 50 mm semi-insulating InP substrate in a DCA MBE system. The substrate (i.e., DRS) temperature, thermocouple temperature, and heater power recorded during the growth of this layer are shown in Fig. 4. The DRS temperature is used to control the setpoint of the thermocouple, which in turn controls the output power of the heater. The supervisory computer checks the DRS temperature every 30 s, and if the DRS temperature has deviated more than ± 1 °C from the substrate setpoint of 460 °C, the computer adds the difference to the thermocouple setpoint. In addition, at the start of growth the thermocouple setpoint is reduced by 6 °C to adjust for the additional radiant heat load of the In and Ga effusion cells.

Using this control algorithm, the substrate temperature tends to stay about 1 °C above its setpoint throughout most of the growth. Decreasing the update time (from 30 to 10 s) and the deviation threshold (from 1.0 to 0.5 °C) would bring the substrate temperature closer to the setpoint. Also, there are small oscillations in the substrate temperature at the start and stop points that are caused by the abrupt changes in the thermal load on the substrate when the In and Ga cells are

opened or closed. In order to improve the feedback control of the substrate temperature, a more sophisticated computer control algorithm such as a proportional–integral–derivative loop could be implemented. In this case the deviation of the substrate temperature from its setpoint would be limited by the noise in the DRS measurement.

As can be seen in Fig. 4, each time the thermocouple setpoint is updated, there is a sharp drop in the heater power and the thermocouple temperature quickly moves to its new setpoint. The thermal response of the thermocouple–heater system is fast compared to the thermal response of the substrate—this is why the nested control loop we are using works so well.

By the end of the growth, the thick InGaAs layer has reduced the DRS signal by a factor of 5. This is indicated by the increase in the noise of the DRS temperature measurement (see Fig. 4). In our experience the DRS technique is limited to the growth of InGaAs layers that are less than 1 μm thick. Also, by the end of the growth the thermocouple temperature is lower than the substrate temperature. The small-band-gap epilayer absorbs a larger part of the heater radiation spectrum than the InP substrate, which is transparent to much of the blackbody spectrum at these temperatures. Therefore, as the InGaAs layer thickens, the transmission losses of heater radiation are reduced, and this reduces both the heater power output and the thermocouple temperature.

If only absorption in the InGaAs layer was important, one would expect the slope of the thermocouple temperature curve to decrease monotonically with thickness. However, a closer look at the thermocouple curve in Fig. 4 shows a slight dip in the slope at a 160 nm layer thickness. This dip is the result of the thin-film interference effects on the emission spectrum in the InGaAs layer. This thin-film interference feature was verified in simulation using the thermal substrate model. It is also interesting to note that for a bare substrate, the initial substrate–thermocouple offset is much lower here than in the previous experiment (30 °C instead of 150 °C). The emission–absorption properties of the thermocouple–heater system of the DCA chamber are very different from those of the VG system used to grow the resonant cavity.

Finally, the spectral dependence of the absorption coefficient of the InGaAs overlayer distorts the shape of the band-edge spectrum. Again, the apparent temperature shift caused by this distortion is corrected using the technique described in Eq. (4). Simulations show that the error is about 2 °C for

a 400 nm thick InGaAs layer and that this apparent temperature shift can be reduced to less than 0.5 °C by using Eq. (4).

V. CONCLUSIONS

A substrate temperature measurement method is presented wherein temperature is inferred from the position of the knee of the band-edge spectrum of the substrate. The width of the knee of the band-edge spectrum is used to correct for spurious shifts in the position of the knee caused by differences in the properties of the substrate and the measurement conditions from those of a reference substrate. Spurious temperature shifts caused by thin-film interference during the growth of a distributed Bragg reflector cavity structure are significantly reduced when using both the position and the width of the knee of the spectrum to determine the temperature. A substrate thermal model is used to predict the key features of the real temperature variations of a radiatively heated substrate during the growth of a $\lambda=930$ nm resonant cavity under constant thermocouple control. Diffuse reflectance spectroscopy is used to control substrate temperature to within ± 2 °C during the growth of the InGaAs on InP. Conventional constant-thermocouple control during the same growth results in substrate temperature variations of more than 50 °C.

ACKNOWLEDGMENTS

This work is part of a DARPA-funded program entitled “Integrated MultiSensor Control of Molecular Beam Epitaxy” under Agreement No. MDA972-95-1-0016, monitored by Lt. Col. Gernot S. Pomrenke.

- ¹S. R. Johnson, C. Lavoie, T. Tiedje, and J. A. Mackenzie, *J. Vac. Sci. Technol. B* **11**, 1007 (1993).
- ²S. R. Johnson, C. Lavoie, M. K. Nissen, and T. Tiedje, U.S. Patent No. 5,388,909 (1995).
- ³J. A. Roth, T. J. DeLyon, and M. E. Adel, *Mater. Res. Soc. Symp. Proc.* **324**, 353 (1994).
- ⁴E. S. Hellman and J. S. Harris, Jr., *J. Cryst. Growth* **81**, 38 (1987).
- ⁵W. S. Lee, G. W. Yoffe, D. G. Schlom, and J. S. Harris, Jr., *J. Cryst. Growth* **111**, 131 (1987).
- ⁶D. M. Kirillov and R. A. Powell, U.S. Patent No. 5,118,200 (1992).
- ⁷S. R. Johnson and T. Tiedje, *J. Cryst. Growth* **175/176**, 273 (1997).
- ⁸S. R. Johnson, Ph.D. thesis, University of British Columbia, 1996.
- ⁹S. R. Johnson and T. Tiedje, *J. Appl. Phys.* **78**, 5609 (1995).
- ¹⁰M. Beaudoin, S. R. Johnson, A. J. G. DeVries, A. Mohades-Kassai, and T. Tiedje, *Mater. Res. Soc. Symp. Proc.* **421**, 367 (1996).
- ¹¹J. A. Roth and A. Bennett, *J. Appl. Phys.* (submitted).
- ¹²B. V. Shanabrook, J. R. Waterman, J. L. Davis, and R. J. Wagner, *Appl. Phys. Lett.* **61**, 2338 (1992).